Deep-Sea Research II 120 (2015) 61–71

Contents lists available at ScienceDirect

Deep-Sea Research II

journal homepage: www.elsevier.com/locate/dsr2

Regional productivity of phytoplankton in the Western Arctic Ocean during summer in 2010

Mi Sun Yun [a], Bo Kyung Kim [a], Hui Tae Joo [a], Eun Jin Yang [b], Shigeto Nishino [c], Kyung Ho Chung [b], Sung-Ho Kang [b], Sang H. Lee [a,*]

[a] Department Oceanography, Pusan National University, 30, Jangjeon-dong, Geumjeong-gu, Busan 609-735, Republic of Korea
[b] Department of Polar Ocean Environment, Korea Polar Research Institute, 26, Songdomirae-ro, Yeonsu-gu, Incheon 406-840, Republic of Korea
[c] Research Institute for Global Change, Japan Agency for Marine-Earth Science and Technology, Yokosuka, Japan

ARTICLE INFO

Available online 10 April 2015

Keywords:
Phytoplankton
Carbon uptake rates
Nitrogen uptake rates
Warm-core eddy
Arctic

ABSTRACT

Phytoplankton production measurements were conducted in the northeast Chukchi Sea and western Canada Basin in the summer season, from 20 July to 10 August 2010, using a ^{13}C–^{15}N dual tracer technique. The daily carbon uptake rate in the northeast Chukchi Sea in 2010 was extremely low, with a mean of 29.8 mg C m^{-2} d^{-1} (SD = 17.6 mg C m^{-2} d^{-1}). Regional and temporal differences caused the low production rate compared to previous studies in the northeast Chukchi Sea. In the western Canada Basin, the mean daily carbon uptake rate from this study was 20.6 mg C m^{-2} d^{-1}, which was influenced by the dominance of small phytoplankton resulting in a low carbon uptake rate in the region. The regionally high nitrate uptake rates compared to ammonium uptake rates in the western Canada Basin can be caused by warm-core eddies, which supply high levels of nitrate to the euphotic zone. Warm-core eddies in the Canada Basin substantially enhanced local phytoplankton production and the contribution of large phytoplankton. Therefore, the effects of physical forcing events (such as "an" eddy) on the primary production need to be examined further to better understand changes of primary production under ongoing environmental changes in the Arctic Ocean.

© 2015 Elsevier Ltd. All rights reserved.

1. Introduction

Over the last decade, the Arctic Ocean has experienced anomalous sea ice loss during summer (Stroeve et al., 2007; Comiso et al., 2008). The sea ice loss creates longer ice-free periods and thus might allow more heating of the upper ocean during summer (Steele et al., 2008). The largest sea ice loss has been observed in the Pacific sector of the Arctic Ocean (Western Arctic Ocean), which is a region that is well matched in both the spatial pattern of sea ice loss and the distribution of warm Pacific Summer Water (PSW) (Shimada et al., 2006). In addition, Steele et al. (2010) found that about 80% of the upper ocean warming in the Pacific sector of the Arctic Ocean during summer originated in local atmospheric heating.

The continuing loss of sea ice could result in changes to various physical environmental factors in the Arctic Ocean. Changes in surface water properties, such as the near-surface temperature maximum (Jackson et al., 2010) and surface ocean acidification (Yamamoto-Kawai et al., 2009), have been observed in the Canada Basin. In addition, a strong Beaufort Gyre (Shimada et al., 2006; Yang, 2009) and thereby the accumulation of surface fresh water within the Beaufort Gyre (Proshutinsky et al., 2009) resulted in the nutricline deepening (McLaughlin and Carmack, 2010) in the Canada Basin. Under the deepened nutricline condition, eddies could have an important role in nutrient transport and phytoplankton distribution (Nishino et al., 2011a, 2013). According to Kawaguchi et al. (2012), eddies may appear more frequently because they are likely to be formed by baroclinic instability of the enhanced westward flow of the Beaufort Gyre associated with the recent loss of sea ice.

These recent environmental changes, caused mainly by the loss of sea ice, have greatly affected the physiological status, community structure, and primary production of phytoplankton (Li et al., 2009; Lasternas and Agustí, 2010; Lee et al., 2010). Li et al. (2009) found the average phytoplankton size to be decreasing in the freshening and warming surface layer in the Canada Basin. Lasternas and Agustí (2010) also reported exceptional dominance of the colonial form of *Phaeocystis pouchetii* following the massive ice losses in summer 2007. In addition, Lee et al. (2010) observed higher carbon and nitrogen uptake rates in phytoplankton with the increased quantity of light passing through thinner sea ice.

Because sea ice loss is strongly related to the increase in underwater irradiance, primary production might be expected to increase in the Arctic Ocean. Based on satellite ocean color data, Arrigo et al.

* Corresponding author. Tel.: +82 51 510 2256; fax: +82 51 581 2963.
E-mail address: sanglee@pusan.ac.kr (S.H. Lee).

http://dx.doi.org/10.1016/j.dsr2.2014.11.023
0967-0645/© 2015 Elsevier Ltd. All rights reserved.

(2008) found that large increases in annual net primary production by phytoplankton on the continental shelves of the Siberian, Laptev, and Chukchi Seas, which can be explained by the increased open water area and a longer growing season. In addition, the increased wind forcing caused by the ice edge retreats can supply deep nutrient-rich waters to the phytoplankton and thus increased primary production on the shelves can be expected (Carmack and Chapman, 2003; Carmack et al., 2004). However, the upper ocean warming and freshening caused by sea ice melting may increase stratification and prevent the nutrient inputs from deep waters to the euphotic zone (Hill et al., 2013). Thus, it is important to monitor how recent phytoplankton production has changed under the rapidly changing environmental conditions in the region of the Arctic Ocean because phytoplankton production could be an important trigger of ecosystem change.

Our first Arctic cruise was conducted onboard the Korean research icebreaker *ARAON* in the Western Arctic Ocean (e.g., Northeast Chukchi Sea and Western Canada Basin) during summer in 2010. Here we describe the general characteristics of phytoplankton production in the region and compare our findings with those of previous studies to improve understanding of changes in primary production under the ongoing environmental changes in the western Arctic Ocean. In addition, the potential effects of an anticyclonic warm-core eddy found in the western Canada Basin on the phytoplankton biomass and production rate are discussed.

2. Materials and methods

2.1. Study area

Oceanographic sampling was undertaken at a total of 38 stations in the northeast Chukchi Sea and the western Canada Basin (mostly in the Chukchi Cap and the west of the Northwind Ridge; Fig. 1) from 20 July to 10 August 2010, onboard the Korean research icebreaker *ARAON*. For deck incubation, primary productivity was measured at 19 selected morning stations (Fig. 1). The study area was comprised of a shallow shelf (< 100 m) and a deep basin (> 3000 m). To understand the regional characteristics of primary productivity, the study area was separated into the northeast Chukchi Sea and the western Canada Basin using 165°W longitude as a boundary. The northeast Chukchi Sea is relatively shallow with a depth of < 100–350 m and contained five productivity stations (Stns. 1, 3, 4, 35, and 38). The productivity stations around the Chukchi Cap and the Northwind Ridge including the western boundary of the Canada Basin were categorized as the western Canada Basin stations (Stns. 6, 8, 10, 13, 14, 16, 18, 21, 23, 27, 28, 29, 31, and 32) (Fig. 1).

2.2. Hydrographic and water sampling

Water column profiles of water temperature, salinity, and density were obtained from downcast measurements using a Seabird SBE-911+ CTD profiler mounted on a rosette. Water samples were collected with the rosette sampler equipped with 20 l Niskin bottles.

The depth of the euphotic zone (Z_{eu}) in this study was defined as the depth receiving 1% of the near-surface PAR value (photosynthetically active radiation) determined using an underwater PAR sensor (LI-COR underwater 4π light sensor), lowered with CTD/rosette sampler. The mixed-layer depth (Z_m) was defined here as the shallowest depth where seawater density first exceeded the value recorded at 5 m depth by 0.03 kg m^{-3} (Gardner et al., 1995).

2.3. Nutrient and chlorophyll a concentration measurements

The discrete water samples used for measurement of dissolved inorganic nutrient concentrations (nitrate, ammonium, phosphate, and silicate) were analyzed onboard immediately after collection, using an automated nutrient analyzer (SEAL, QuAAtro) following

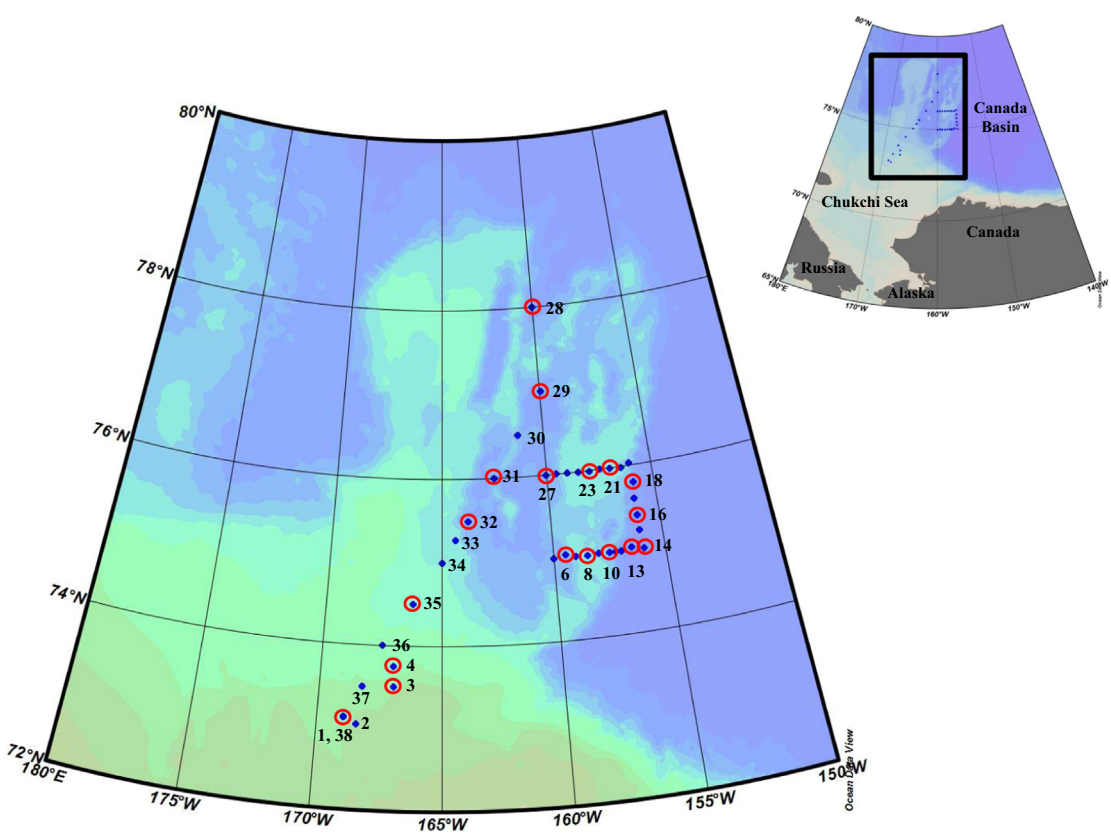

Fig. 1. Locations of the primary productivity stations during the 2010 *ARAON* cruise in the northeast Chukchi Sea and western Canada Basin. Location of st. 38 represents a revisit of st. 1.

the QuAAtro multitest methods. The analytical accuracy for nutrient concentrations in water samples was ±0.02 μM for phosphate and ±0.1 μM for nitrite+nitrate, ammonium, and silicate.

Water samples used for the measurement of total chlorophyll *a* concentration were filtered through Whatman GF/F filters (24 mm). The size-fractionated chlorophyll *a* concentration was determined for samples passed sequentially through 20- and 5-μm Nuclepore filters (47 mm) and 0.7-μm Whatman GF/F filters (47 mm). The filters were kept frozen until the analysis onboard. The filters were subsequently extracted in 90% acetone, placed in a freezer at 4 °C for 24 h, and centrifuged following the procedure of Parsons et al. (1984). Chlorophyll *a* concentrations were measured using a Trilogy fluorometer (Turner Designs, USA) which had been calibrated with commercially purified chlorophyll *a* preparations.

2.4. Phytoplankton uptake rate measurements using stable carbon and nitrogen isotopes

In situ carbon and nitrogen uptake rates of phytoplankton were measured using a ^{13}C–^{15}N dual tracer technique (Lee and Whitledge, 2005; Lee et al., 2010). Six photic depths (100%, 50%, 30%, 12%, 5%, and 1% penetration of near-surface irradiance, PAR) were determined from the underwater PAR sensor (LI-COR underwater 4π light sensor) lowered with CTD/rosette sampler. The near-surface PAR (100% light depth) was measured at 2 m depth just below the ocean surface. Water samples were collected from all of the corresponding light depths to use in the on deck incubations and the surface water collected from 2 m depth was used for 100% light treatment. Water samples were screened through a 300-μm Nitex mesh to remove large grazers (Sakshaug, 1980; Carmack et al., 2004) and taken in polycarbonate incubation bottles (0.5 L), which were covered with neutral density screens to simulate each light depth over the euphotic zone. Labeled carbon ($NaH^{13}CO_3$), nitrate ($K^{15}NO_3$), and ammonium ($^{15}NH_4Cl$) substrates were inoculated in the bottles immediately after water sampling. Bottles were incubated on deck in a large polycarbonate incubator cooled with running surface seawater under natural light conditions for approximately 4 to 5 h. After the incubation, all samples used to determine productivity were terminated by low-vacuum (<100 mm Hg) filtration onto precombusted (450 °C, 4 h) glass fiber filters (Whatman GF/F; diameter=25 mm) and then immediately frozen at −20 °C. In home laboratory, the frozen filters were acidified by concentrated hydrochloric acid (HCl) fumes overnight to remove carbonate (Hama et al., 1983). After HCl fume treatment, the filters were almost dried up. The abundances of ^{13}C and ^{15}N and the total amounts of particulate organic carbon (POC) and nitrogen (PON) were determined using the Thermo Finnigan Delta+XL mass spectrometer at the Alaska Stable Isotope Laboratory of the University of Alaska, Fairbanks, USA. Finally, the carbon and nitrogen production rates were calculated based on Hama et al. (1983) and Dugdale and Goering (1967), respectively. All carbon and nitrogen uptake rates were expressed as multiplying specific uptake rates (carbon or nitrogen taken up per unit particulate organic carbon or nitrogen) by particulate organic matter concentrations.

3. Results

3.1. Physical condition

The water mass distribution in the western Arctic Ocean was characterized by the inflow of Pacific Water through the Bering Strait. Pacific Summer Water (PSW) and Pacific Winter Water (PWW) in the upper layers of the western Arctic Ocean (<~200 m) are shown in Fig. 2. In the upper 200 m, the temperature ranged from −1.7 to 0.5 °C. Temperature maximums of −1.0–0.5 °C were observed between 50 and 100 m and were linked to the inflow of PSW, while a temperature minimum (<−1.4 °C) between 100 m and 200 m was linked to the injection of PWW (Fig. 2a). Salinity in the upper 200 m ranged from 25.5 to 34 psu and surface salinity was lowest owing to summer sea ice melt, river runoff, and low-salinity PSW (Fig. 2b). The upper halocline (characterized by a salinity of 33.1) had a near-freezing temperature minimum and nutrient maximum (e.g., Jones and Anderson, 1986; Cooper et al., 1997). According to Pickart and Stossmeister (2008), the eastward-flowing shelfbreak boundary current advected this upper halocline water and their seasonally different configurations lead to the formation of different types eddies in the Canada Basin.

The Z_{eu} varied between 30 and 60 m among the production stations with a mean of 48±8 m (Table 1). The mixed layer occupied the 7–23 m depth range. At the stations with low levels of sea ice cover (<40%), the mean Z_m was shallow, extending only to a depth of 9 m. In comparison, a thicker mixed layer (mean=13 m) was observed at the heavy ice covered stations (>50%) (Table 1).

3.2. Nutrient distribution

In the study area, the nitrate concentrations of surface waters were low (<1 μM), but rapidly increased with increasing depth (Fig. 3a). The nitrate concentration within the Z_{eu} ranged from 0.36

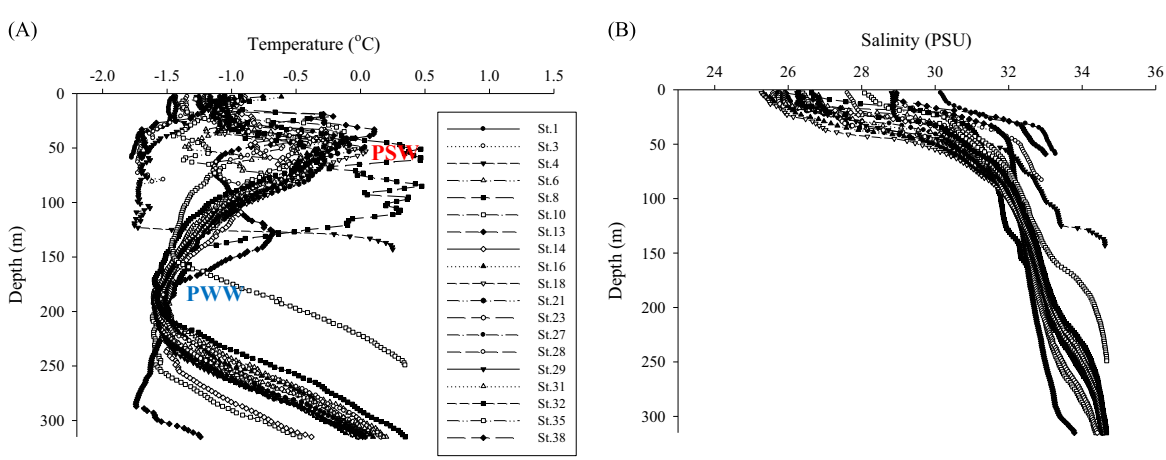

Fig. 2. The vertical structure of temperature [°C] (a) and salinity (b) in the study area in 2010.

Table 1
Location, water depth (m), euphotic zone depth (Z_{eu}), mixed layer depth (Z_m), and sea ice cover (%) for phytoplankton productivity stations in the northeast Chukchi Sea and western Canada Basin in 2010.

Station	Date (mm/dd/yr)	Location		Depth (m)	Z_{eu} (m)	Z_m (m)	Sea ice coverage (%)
		Latitude (°N)	Longitude (°W)				
1	07/20/10	73.1263	168.9477	75	30	11	80–90
3	07/21/10	73.5107	166.9910	110	40	13	60–70
4	07/23/10	73.7467	167.0553	165	40	23	80–90
6	07/26/10	75.0422	159.4983	1840	42	9	0–10
8	07/27/10	74.9930	158.4880	950	40	9	20–30
10	07/27/10	75.0130	157.4958	1290	50	9	10–20
13	07/28/10	75.1987	156.3967	3900	44	9	70–80
14	07/29/10	74.9753	155.9090	3904	50	9	0–10
16	07/30/10	75.4442	156.0717	2800	60	9	10–20
18	07/31/10	75.7943	155.9358	2050	60	9	20–30
21	08/01/10	75.9912	156.9975	940	54	13	70–80
23	08/01/10	75.9935	157.9603	520	54	15	50–60
27	08/02/10	75.9870	160.1027	2100	56	9	20–30
28	08/06/10	78.0040	160.0302	2660	44	7	70–80
29	08/07/10	76.9980	159.9532	2160	60	13	70–80
31	08/07/10	75.9903	162.5230	2090	53	13	0–10
32	08/08/10	75.4995	163.8303	1920	50	9	10–20
35	08/09/10	74.5065	166.2580	340	46	7	30–40
38	08/10/10	73.1165	168.9323	73	38	9	0–10

to 4.18 μM, with a mean of 0.93 μM (SD= ± 0.90 μM), whereas the nitrate concentration within the Z_m ranged from 0 to 0.86 μM, with a mean of 0.30 μM (SD= ± 0.21 μM). The ammonium concentration was fairly uniform throughout the water column, except for some stations (Fig. 3b). The concentration of phosphate in surface waters was about 0.5 μM and reached up to 2.0 μM throughout the water column (Fig. 3c). The vertical distribution of silicate concentrations in the upper 300 m was very similar to that of nitrates and they were generally higher in the bottom layer than in the shallow layers (Fig. 3d).

3.3. Chlorophyll a concentration

The chlorophyll *a* concentration integrated from surface to mixed-layer depth ranged from 0.2 to 2.4 mg m^{-2}, with a mean of 0.6 mg m^{-2} (SD=0.6 mg m^{-2}) (Fig. 4). The averaged concentrations up to mixed- layer depth were 1.3 mg m^{-2} (SD= ± 0.7 mg m^{-2}) and 0.3 mg m^{-2} (SD= ± 0.2 mg m^{-2}) for the northeast Chukchi Sea and the western Canada Basin, respectively. The chlorophyll *a* concentration integrated over the euphotic zone averaged for all the productivity stations was 8.3 mg m^{-2} (SD= ± 5.0 mg m^{-2}). In the northeast Chukchi Sea, the average chlorophyll *a* concentration was 9.7 ± 3.7 mg m^{-2}. In comparison, the chlorophyll *a* concentration in the western Canada Basin was 7.7 mg m^{-2} (SD= ± 5.4 mg m^{-2}). Remarkably high chlorophyll *a* concentrations (> 15 mg m^{-2}) were observed at stations 10 and 13 in the western Canada Basin, even when other stations in the region showed evenly low chlorophyll *a* concentrations (Fig. 4).

The percentage of the total chlorophyll *a* concentration in the different size fractions for each of the 19 stations is shown in Fig. 5. On average, the large phytoplankton (> 20 μm) contributed about 26.2% (SD= ± 20.8%), whereas the small phytoplankton (0.7–5 μm) contributed 54.8% (SD= ± 21.7%) of the total chlorophyll *a* concentration in the study area. Medium-size phytoplankton (5–20 μm) contributed about 19.0% (SD= ± 11.0%). With the exception of station 35, the contribution of large and medium-size phytoplankton (> 5 μm) was considerably higher in the northeast Chukchi Sea (over 70%), whereas the small phytoplankton contributed about 70% of the total biomass in the western Canada Basin. At stations 10 and 13, the contribution of large and medium-size phytoplankton (> 5 μm) was remarkably high (up to 55%) and the contribution of small phytoplankton was low (about 45%) (Fig. 5).

3.4. Vertical patterns of chlorophyll a, primary production, and biomass-specific production

The chlorophyll *a* concentration was lowest at the surface, with a mean of 0.06 mg m^{-3} (SD= ± 0.04 mg m^{-3}) and the maximum concentration of chlorophyll *a* was 0.63 mg m^{-3} (SD= ± 0.57 mg m^{-3}) at 1% light level in this study (Fig. 6). The productivity maximum was also observed at 1% light level with a mean 0.06 mg C m^{-3} h^{-1} (SD= ± 0.10 mg C m^{-3} h^{-1}). It seems that the maximum productivity occurred in association with the chlorophyll *a* maximum. The highest biomass-specific production was observed at the surface, decreasing with depth (Fig. 6). The biomass-specific productions were not significantly different (*t*-test, $p > 0.05$) between the northeast Chukchi Sea and western Canada Basin.

3.5. Carbon and nitrogen uptake rates

Hourly carbon uptake rates integrated over the euphotic zone from six light depths ranged from 0.17 to 4.15 mg C m^{-2} h^{-1}, with a mean of 0.96 mg C m^{-2} h^{-1} (SD=0.98 mg C m^{-2} h^{-1}) (Fig. 7). The carbon uptake rates in the northeast Chukchi Sea ranged from 0.37 to 2.24 mg C m^{-2} h^{-1}, with a mean of 1.24 mg C m^{-2} h^{-1} (SD= ± 0.73 mg C m^{-2} h^{-1}). In comparison, the average rates in the western Canada Basin were slightly lower than that in the northeast Chukchi Sea (0.86 ± 1.06 mg C m^{-2} h^{-1}). Although the rates at other stations in the western Canada Basin were low (< 1 mg C m^{-2} h^{-1}), stations 10 and 13 had exceptionally high values (Fig. 7).

Total nitrogen (nitrate+ammonium) uptake rates ranged from 0.24 mg N m^{-2} h^{-1} to 7.50 mg N m^{-2} h^{-1}, with a mean of 2.0 mg N m^{-2} h^{-1} (SD= ± 2.3 mg N m^{-2} h^{-1}) (Fig. 8). The vertically integrated nitrate uptake rates ranged from 0.02 mg NO_3 m^{-2} h^{-1} to 5.15 mg NO_3 m^{-2} h^{-1} (mean ± SD=0.9 ± 1.5 mg NO_3 m^{-2} h^{-1}), whereas the ammonium uptake rates ranged from 0.08 mg NH_4 m^{-2} h^{-1} to 6.90 mg NH_4 m^{-2} h^{-1}, with a mean of 1.1 mg NH_4 m^{-2} h^{-1} (SD= ± 1.5 mg NH_4 m^{-2} h^{-1}). The average nitrate uptake rate was 1.3 mg NO_3 m^{-2} h^{-1} (SD= ± 1.6 mg NO_3 m^{-2} h^{-1}) in the northeast Chukchi Sea, whereas the average nitrate uptake rate in the western Canada Basin was 0.8 mg NO_3 m^{-2} h^{-1} (SD= ± 1.5 mg NO_3 m^{-2} h^{-1}). In comparison, the average ammonium uptake rates for the northeast Chukchi Sea and western Canada Basin were 1.9 mg NH_4 m^{-2} h^{-1} (SD= ± 2.8 mg NH_4 m^{-2} h^{-1}) and 0.8 mg NH_4 m^{-2} h^{-1} (SD= ± 0.6 mg NH_4 m^{-2} h^{-1}), respectively. Stations 10 and 13 in the western Canada Basin had considerably higher nitrate uptake rates compared to ammonium uptake rates, unlike the other stations, which had higher ammonium uptake rates or similar nitrate and ammonium uptake rates (Fig. 8). The nitrate uptake rates in this region (stations 10 and 13) were about two orders of magnitude higher than those in other stations in the western Canada Basin.

3.6. Warm-core eddies in the Canada Basin

In a transect from stations 5 to 14 within the western Canada Basin, warm-core eddies were observed near the surface to a depth of 100 m (Fig. 9a). The geostrophic velocity indicated that two warm eddies were spinning anticyclonically (Fig. 9b). The core temperature reached about −0.5 °C in the two warm eddies. The diameters of the eddies were approximately 25 km and 40 km in the horizontal axis for the left and right sides of the eddies, respectively, and slightly larger than the scale of previously

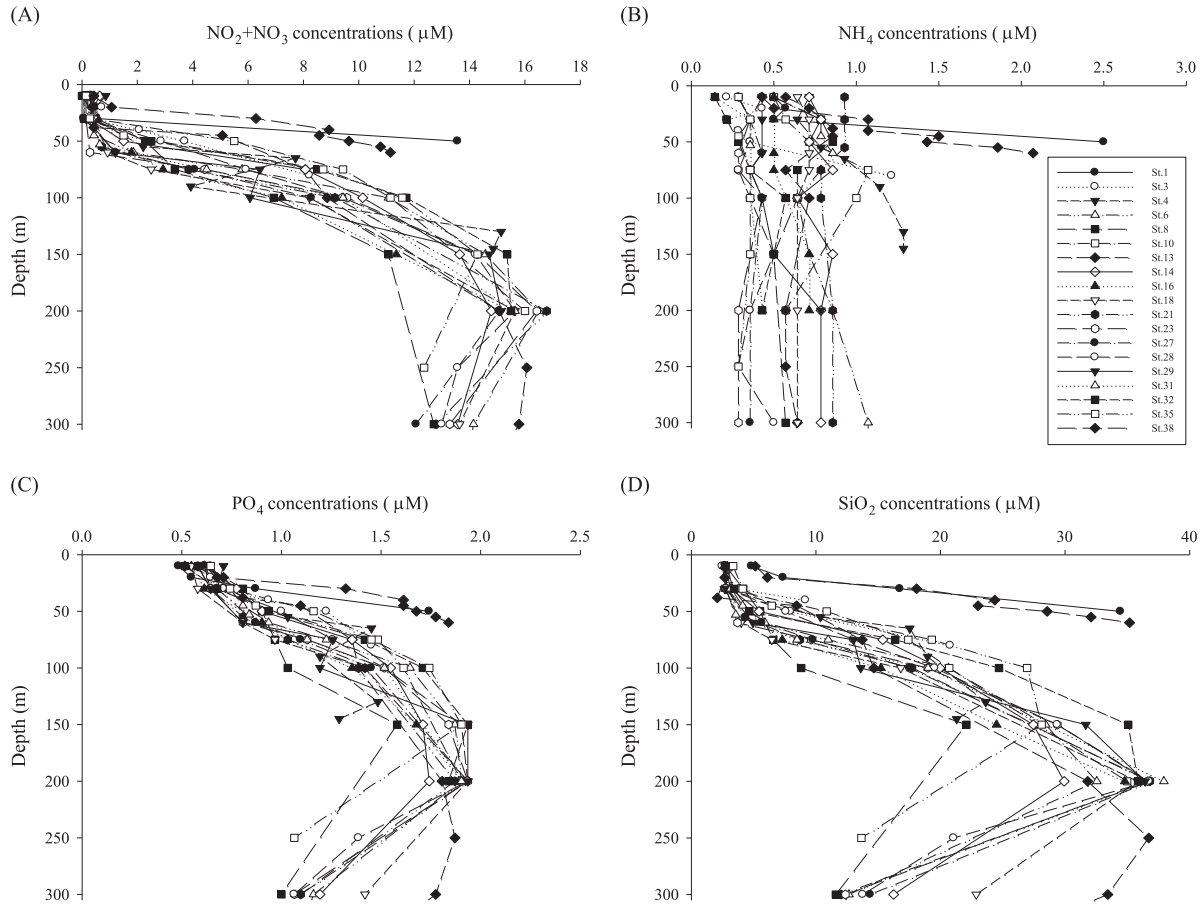

Fig. 3. The vertical structure of nitrate [μmol/l] (a), ammonium [μmol/l] (b), phosphate [μmol/l] (c), and silicate [μmol/l] (d) concentrations in the study area in 2010.

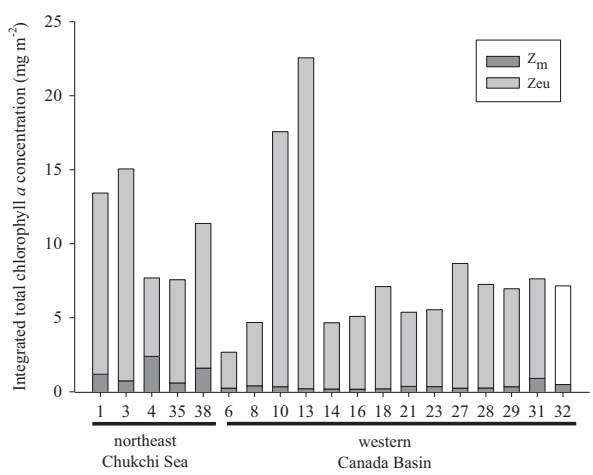

Fig. 4. Total chlorophyll *a* concentrations [mg m^{-2}]. The chlorophyll *a* data were obtained by the integration of volumetric values from the surface to 1% light depth.

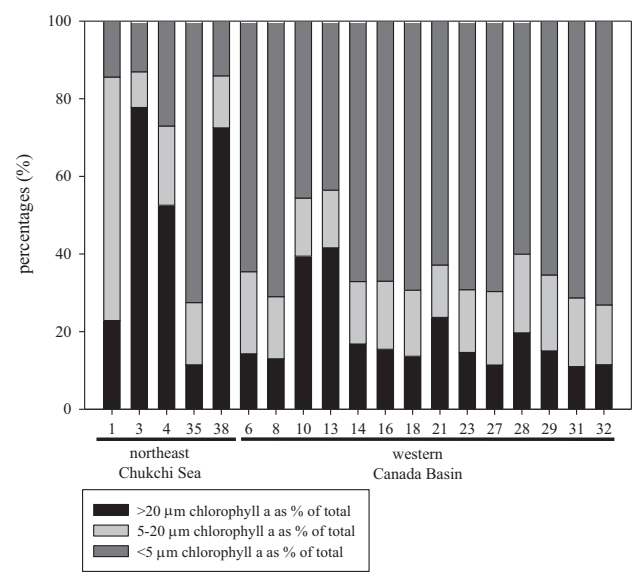

Fig. 5. Percentage of chlorophyll *a* in the different size fractions (> 20 μm, 5–20 μm, and < 5 μm) for each of the 19 primary production stations.

reported eddies (10–20 km) (Muench et al., 2000; Mathis et al., 2007; Pickart and Stossmeister, 2008). The cold water with salinity of 33 and 34 was identified as PWW located below the surface warm water (Fig. 9a).

A depressed nitracline was observed below the core of the left side eddy, while the shoaling of the nitracline with the right side eddy was shown in between two eddies (Fig. 9c). The silicate and phosphate distributions were similar to those of nitrate (data not shown), whereas the mean ammonium concentration in eddy regimes was not largely different from that in other stations of the Canada Basin (detailed in Section 4.3). Chlorophyll *a* concentrations were higher at the periphery of the eddies than in the surrounding waters at the same depths (Fig. 10a). The highest chlorophyll *a* concentrations were observed at stations 10 and 13. On the basis of the size-fractionated chlorophyll *a* concentration, we identified that the contribution of large phytoplankton (> 20 μm) at stations 10 and 13 was high (up to 40%) compared to the other stations, which had lower contributions from large phytoplankton (about 15% of total biomass) (Fig. 10b).

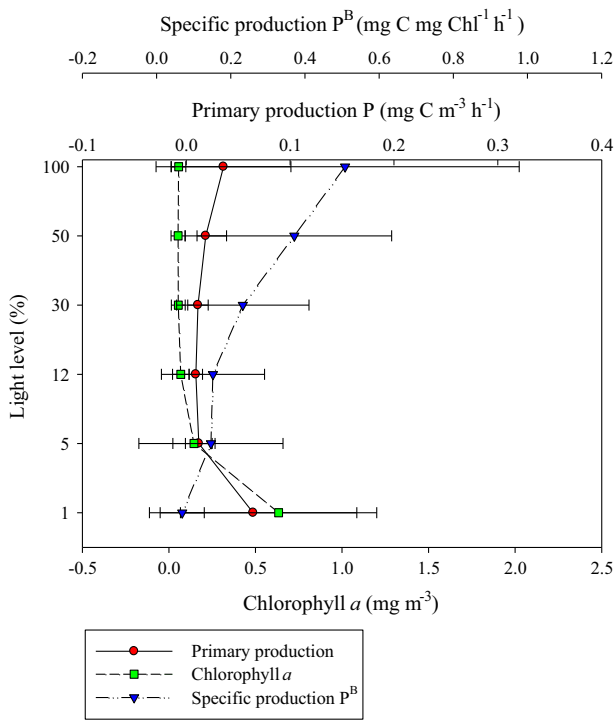

Fig. 6. Vertical distributions of chlorophyll *a*, primary production, and biomass-specific production at 19 primary production stations during summer in 2010. Values shown are means ± sd.

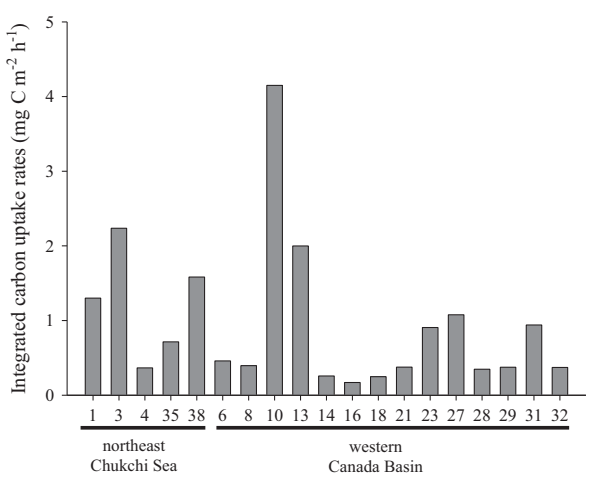

Fig. 7. Hourly carbon uptake rates [mg C m^{-2} h^{-1}] integrated from the surface to 1% light depth.

4. Discussion

4.1. Carbon uptake rate

4.1.1. Carbon uptake rate in the northeast Chukchi Sea

Based on a 24-h photo period (Subba Rao and Platt, 1984) and the hourly carbon uptake rates measured in this study, the mean daily carbon uptake rate of phytoplankton was 29.8 mg C m^{-2} d^{-1} in the northeast Chukchi Sea. This value is very low compared with those reported from previous studies in the region (Table 2). Lee et al. (2013a) reported about six-times higher carbon uptake rates in the northern Chukchi Sea (mean = 175.5 mg C m^{-2} d^{-1}). In addition, the daily carbon uptake rates obtained by Yun et al. (2014) and Lee et al. (2007) were 135.9 mg C m^{-2} d^{-1} and 162 mg C m^{-2} d^{-1} in the northern Chukchi Sea, which is located primarily around Wrangel Island.

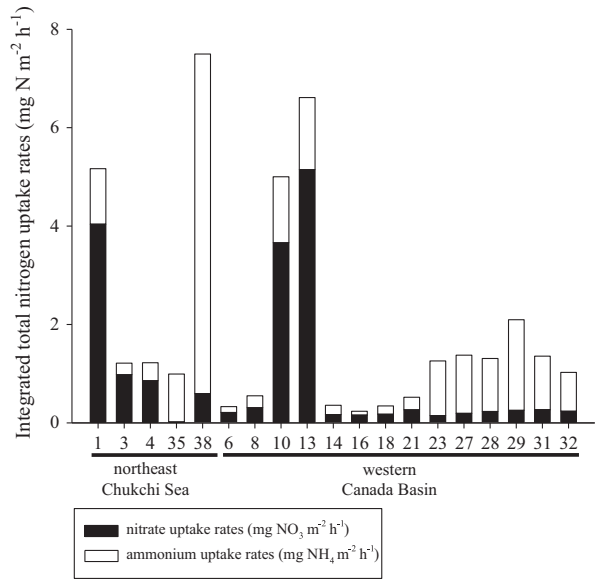

Fig. 8. Hourly total nitrogen uptake rates [mg N m^{-2} h^{-1}] integrated from the surface to 1% light depth.

The extremely low rate in this study compared to previous studies might be explained by regional differences. The study regions of Lee et al. (2007) and Yun et al. (2014) were located in the western part of the northern Chukchi Sea, which is strongly affected by Anadyr Water carrying high nutrients and phytoplankton biomass (Robie et al., 1992; Springer and McRoy, 1993), whereas the region we studied was mainly in the eastern part of the northern Chukchi Sea. In fact, because of the different water masses in the Chukchi Sea, largely different primary productions in the western and eastern sides have been identified in some studies (Walsh et al., 1989; Lee et al., 2007; Yun et al., 2014). Although the region investigated by Lee et al. (2013a) covered the eastern part of the Chukchi Sea, it was located at a lower latitude (< 72°N) than our study region (72°N–75°N). According to Gosselin et al. (1997), average areal rates of particulate production sharply decrease with increasing latitude between 70°N and 75°N. They suggested that the latitudinal variability of phytoplankton production and biomass in summer were regulated by the surface ice cover and the surface mixed-layer depths, since they determine the amount of light available to the phytoplankton in the water column (Gosselin et al., 1997). Thus, the lower carbon uptake rate in this study compared to previous studies can be due to the high latitudinal location with easterly location.

In addition to regional differences, temporal differences might affect the carbon uptake rate of phytoplankton. Previous studies were usually conducted in August or September (Lee et al., 2007, 2013a; Yun et al., 2014) (Table 2), which presented generally ice-free or sparse ice conditions in the Chukchi Sea. However, our study was conducted during the early ice-opening season. Considerable ice cover was present during the expedition in the Chukchi Sea except for at station 38, which was the final station of the cruise (See Table 1). Based on satellite data, we observed that most of the study area in July was completely covered by heavy ice with a concentration over 70%. Ice cover started to retreat from the region towards August and was covered by partially melted and fragmented ice. Assuming open water for the region where sea ice cover was lower than 30% as suggested by Hill et al. (2013), approximately 26% was occupied as open water area within the entire area in July and open water area in mid-August was increased up to about 49%. Since the greater ice cover would cause slower phytoplankton growth and reduced biomass, the lower carbon uptake rate in our study compared to previous

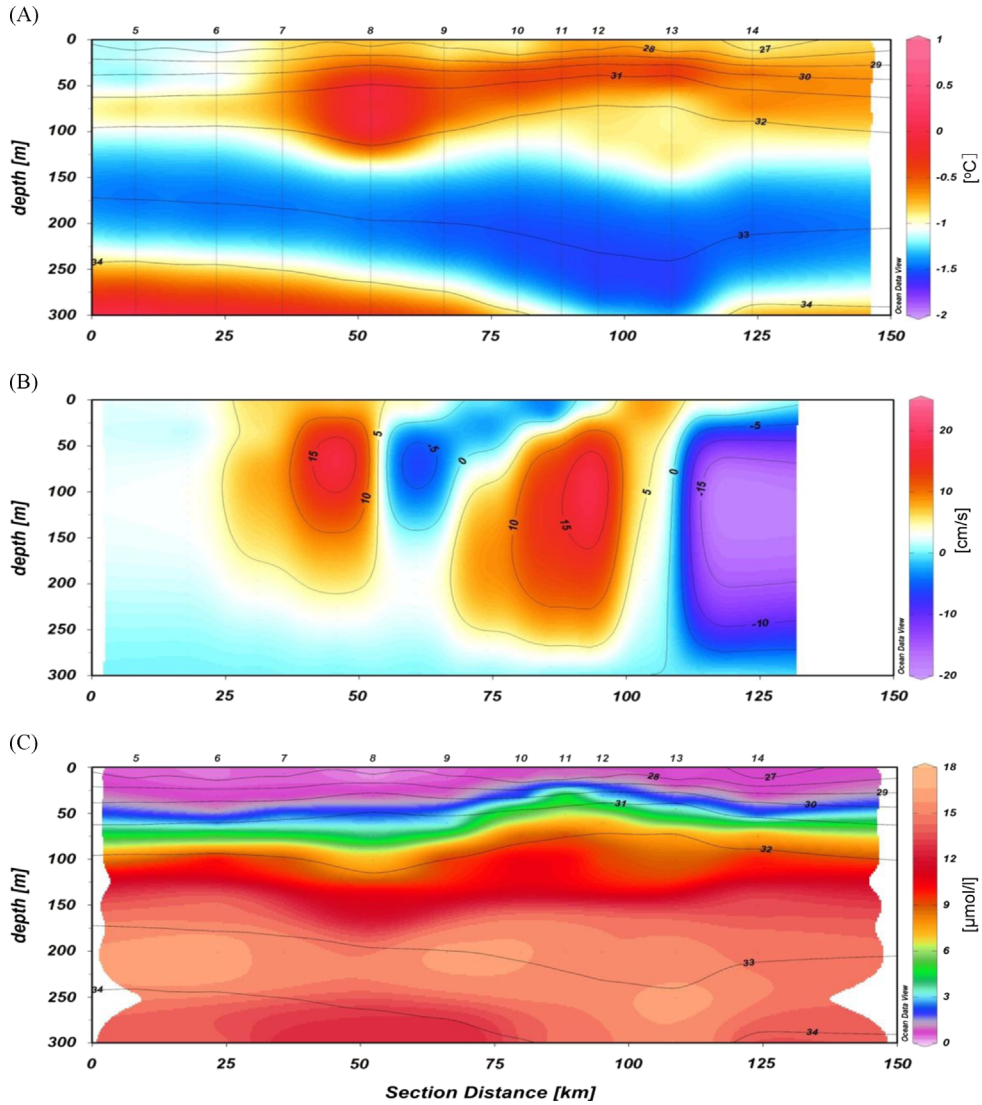

Fig. 9. Vertical sections of temperature [°C] (color) and salinity (contours) (a), geostrophic velocity [cm/s] (b), and nitrite and nitrate concentrations [μmol/l] (c) along a section from station 5 to station 14 in the western Canada Basin. Geostrophic velocity was calculated assuming that the level of no motion lies at 300 db.

studies could be induced under the greater ice cover generating a weak light regime. Yun et al. (2012) found lower specific carbon uptake rates (h^{-1}) (carbon taken up per unit particulate organic carbon: therein Legendre and Gosselin, 1996) under heavy ice cover compared to ice-free and intermediate conditions.

In addition, the phytoplankton in some locations had already experienced the bloom phase and thus caused low carbon uptake rates during this study. Vertical profiles of chlorophyll *a* and productivity showed that they were considerably low in the surface waters and the maximum productivity occurred in association with the chlorophyll *a* maximum depth, which is corresponding to 1% light depth (Fig. 6). The nitrate data indicated the concentrations within Z_m and Z_{eu} was very low as 0.30 ± 0.21 μM and 0.93 ± 0.90 μM, respectively. These general distributions of chlorophyll *a* and nitrate suggest a post-bloom condition (Cota et al., 1996). Although the considerable sea ice cover existed during this study, the phytoplankton could have bloomed under the thin ice or ice free conditions. However, some locations might not yet have experienced a bloom under the heavy ice conditions or just started a bloom-phase with early ice-opening. Therefore, the sea ice cover could be a major factor affecting carbon uptake rates during this study.

4.1.2. Carbon uptake rate in the western Canada Basin

The average daily carbon uptake rate in the western Canada Basin from this study was 20.6 mg C m^{-2} d^{-1} (based on a 24-h photoperiod for comparison with previous studies). This value includes the exceptionally high carbon uptake rates at stations 10 and 13, which were affected by warm-core eddies (detailed in Section 4.3). Lee and Whitledge (2005) reported a mean daily carbon uptake rate of 106 mg C m^{-2} d^{-1} in the western Canada Basin during mid-August to early September. Lee et al. (2010) obtained carbon uptake rates (59.5 mg C m^{-2} d^{-1}) during late June to mid-July that were three times higher than the values in our study (Table 2). In addition, Lee et al. (2012) reported mean daily carbon uptake rates of 31.2 mg C m^{-2} d^{-1} and 74.4 mg C m^{-2} d^{-1} for ice-free and newly open regions, respectively in the Canada Basin during early August to early September. The daily carbon uptake rates under an ice-covered region, estimated by Yun et al. (2012) based on mid-September to mid-October measurement, were lower (9.8 mg C m^{-2} d^{-1}) than the values in this study. If the substantially high values at stations 10 and 13 are not considered, the value in this study (11.9 ± 7.3 mg C m^{-2} d^{-1}) is comparable with that obtained by Yun et al. (2012).

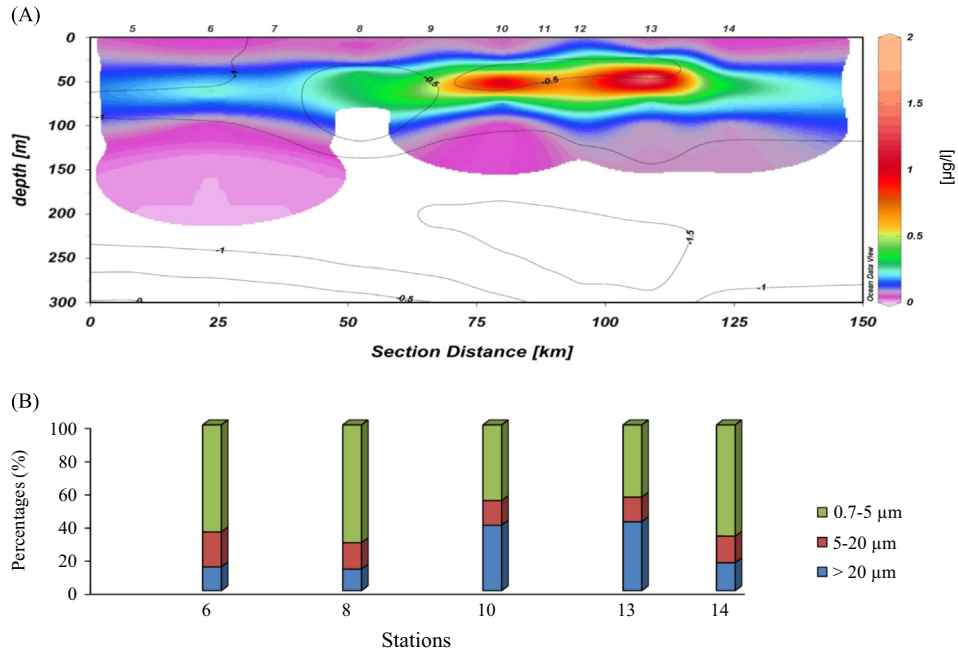

Fig. 10. Vertical sections of chlorophyll *a* concentrations [μg/l] (color) and temperature [°C] (contours) (a) along a section from station 5 to station 14 in the western Canada Basin. Percentages of chlorophyll *a* in the different size fractions (> 20 μm, 5–20 μm, and < 5 μm) (b) were obtained from five stations.

Table 2
Comparison of recent daily carbon uptake rates measured using ^{13}C–^{15}N dual stable isotopes and integrated chlorophyll *a* concentrations in the northern Chukchi Sea and Canada Basin.

Region	Place	Source	Daily carbon uptake rates (mg C m^{-2} d^{-1})	Integrated chlorophyll *a* concentration (mg m^{-2})	Season
Northern Chukchi Sea	western part	Lee et al. (2007)	162	126	From 10 to 22 Aug
	western part	Yun et al. (2014)	135.9	25.4	From 1 to 31 Sep
	southeast part	Lee et al. (2013a)	175.5	26	From 5 to 14 Aug
	northeast part	**This study**	29.8	9.7	From 20 July to 10 August
Canada Basin	western part	Lee and Whitledge (2005)	106	7.3	From mid Aug to early Sep
	western part	Lee et al. (2010)	59.5	10.8	From 27 Jun to 26 Jul
	western part (ice-free region)	Lee et al. (2012)	31.2	13.8	From1 Aug to 7 Sep
	western part (newly opened region)	Lee et al. (2012)	74.4	11.8	From1 Aug to 7 Sep
	central part	Yun et al. (2012)	9.8	6.03	From Sep 17 to 15 Oct
	western part	**This study**	20.6	7.7	From 20 July to 10 August

Although each study was executed in different summer seasons, phytoplankton biomass represented as chlorophyll *a* was not largely different among studies (Table 2). In contrast, the production/biomass ratio (P/B ratio which was calculated by dividing the daily carbon production rate (mg C m^{-2} d^{-1}) by the integrated chlorophyll a concentration (mg chl m^{-2}) was considerably different among studies. For example, Lee and Whitledge (2005) obtained the highest P/B ratio (14.5) during mid-August to early September, and then Lee et al. (2012) reported the second-highest P/B ratio (6.3) based on the measurement from 1 August to 7 September. Lee et al. (2010) found a lower P/B ratio (5.5) during the early summer from late June to mid-July. We obtained a much lower P/B ratio (2.7), and Yun et al. (2012) found the lowest ratio (1.6) during mid-September to mid-October in 2009. This is similar to the sequence of daily carbon uptake rates to our study. Thus, the different biomass-specific photosynthetic rate in different seasons might be one of factors affecting the carbon uptake rates of phytoplankton in the Canada Basin.

Since the carbon uptake rates of phytoplankton could be different by phytoplankton size composition (Lee et al., 2013b), the size composition of phytoplankton might affect to the phytoplankton production in the region. In our study, as much as 64% (SD=9.1%) of phytoplankton was small (0.7–5 μm), and large phytoplankton (> 20 μm) did not exceed 20% (SD=9.9%) of the total biomass (Fig. 5). The high carbon and nitrogen uptake rates of phytoplankton at stations 10 and 13 in the Canada Basin coincided with a dominance of large phytoplankton (about 40.5%), suggesting that the high levels of small phytoplankton observed in this study may be associated with the low carbon uptake rate. In fact, there was a positive relationship between the large size phytoplankton fraction and carbon uptake rates (r^2=0.59, p < 0.05). In the southern Chukchi Sea, Lee et al. (2013b) reported that small phytoplankton had lower specific carbon uptake rates compared to large phytoplankton. Therefore, the amount of large cell contribution appears to be a major determinant of greater productivity in the region and consequently the low carbon uptake rates in the

western Canada Basin observed in this study may be the result of the dominance of small phytoplankton with a low uptake rates (Lee et al., 2013b).

4.2. Nitrogen uptake rate in 2010

The mean daily nitrate uptake rates of phytoplankton in the northeast Chukchi Sea and western Canada Basin in 2010 were 31.2 mg NO_3 m^{-2} d^{-1} (SD=37.8 mg NO_3 m^{-2} d^{-1}) and 19.6 mg NO_3 m^{-2} d^{-1} (SD=37.2 mg NO_3 m^{-2} d^{-1}), respectively. In comparison, the mean daily ammonium uptake rates of phytoplankton were 46.1 mg NH_4 m^{-2} d^{-1} (SD=67.5 mg NH_4 m^{-2} d^{-1}) and 18.8 mg NH_4 m^{-2} d^{-1} (SD=14.3 mg NH_4 m^{-2} d^{-1}) for the northeast Chukchi Sea and western Canada Basin, respectively. Higher uptake rates of ammonium than nitrate by phytoplankton were observed in the northeast Chukchi Sea, whereas in the western Canada Basin, nitrate uptake rates were slightly higher than ammonium uptake. In some previous studies in the Canada Basin, nitrogen uptake rates of phytoplankton were usually dependent on ammonium (Lee and Whitledge, 2005; Lee et al., 2010; Yun et al., 2012). Those studies reported ammonium uptake rates that were three to seven times higher than the nitrate uptake rates (Lee and Whitledge, 2005; Lee et al., 2010; Yun et al., 2012). The noticeably high nitrate uptake rates compared to ammonium uptake rates observed in some stations of the Canada Basin in our study might be the result of the increased nitrate uptake rate as a consequence of nitrate supply by warm-core eddies (detailed in Section 4.3). The nitrate input to the euphotic zone could have resulted in enormously high nitrate uptake rates by phytoplankton in the western Canada Basin in 2010 (Fig. 8). The average nitrate uptake rate calculated after excluding stations 10 and 13 in the eddy regime was 5.2 mg NO_3 m^{-2} d^{-1}, which is about three times lower than the ammonium uptake rate (16.3 mg NH_4 m^{-2} d^{-1}).

In our study, the mean *f*-ratio (nitrate uptake/nitrate+ammonium uptakes) was 0.39 (SD=0.21) in the western Canada Basin. This value is considerably high, compared with those reported in previous studies in the region (Cota et al., 1996; Lee and Whitledge, 2005; Yun et al., 2012). Cota et al. (1996) found that the mean *f*-ratio was 0.12 in the Canada Basin. The ratios (0.25 and 0.22) obtained by Lee and Whitledge (2005) and Yun et al. (2012) in the Canada Basin were lower than our result. However, some stations (stations 23–32) in the Canada Basin showed a low *f*-ratio (about 0.2) and this value is comparable with those of previous studies. Thus, the *f*-ratio from our study could be decreased if there were no effects of eddies in the region.

The hourly nitrate uptake rate in the Canada Basin in our study (0.2 mg N m^{-2} h^{-1} excluding stations 10 and 13) was about twice as high as the rate (0.1 mg N m^{-2} h^{-1}) obtained in 2009 by Nishino et al. (2011b). This difference might have been induced by variations in the strength of the Beaufort Gyre. According to Nishino et al. (2011b), accumulation of fresh water within the Beaufort Gyre (McLaughlin and Carmack, 2010; Nishino et al., 2011b) produces a density gradient between the shelf and basin, resulting in the formation of a strong westward flow over the shelf slope. In 2008/2009, this strong westward flow inhibited phytoplankton growth and reduced the efficiency of the biological pump in the Canada Basin, preventing the spread of nutrient-rich shelf waters towards the Canada Basin (Nishino et al., 2011b). The Beaufort Gyre has recently been enhanced by the melting of thick and solid multiyear ice, which has produced fragmented and mobile sea ice allowing the wind to drive the ocean circulation more effectively (Shimada et al., 2006; Yang, 2009). In addition, Nishino et al. (2013) reported that the Beaufort Gyre was substantially enhanced in 2008–2010 compared to 2002/2003. However, the Beaufort Gyre was slightly reduced in 2010 compared to 2009 (see Nishino et al., 2013) which might have resulted in higher nitrogen production of phytoplankton in the Canada Basin in 2010 compared to 2009. Based on the observations of sea ice condition and fresh water content in the Beaufort Gyre over the last 10 years, Krishfield et al. (2014) reported that the magnitude of total fresh water in Beaufort Gyre in summer steadily increased with peaking in 2010 and afterward slightly has declined. Their findings suggest that the ocean anticyclonic circulation regime is weakening, which is resulting in net export of fresh water from the region. Thus, more observations are need to identify how the variations of total fresh water content in the Beaufort Gyre influence the stratification and gyre circulation pattern and consequently change the primary production in the region.

4.3. The effects of warm-core eddies on the phytoplankton biomass and production rate

The eddies observed during our study were sub-surface anticyclonic warm-core eddies (50–100 m) containing Chukchi Summer Water (see Pickart and Stossmeister, 2008). Pickart and Stossmeister (2008) suggested that these sub-surface warm eddies are probably formed when the shelf-break jet has been replaced with PSW, which is warmer summertime Chukchi Sea shelf water. According to Pickart and Stossmeister (2008), the most common type of eddy found in the Canada Basin is a sub-surface anticyclonic cold-core eddy (100–200 m) containing weakly stratified PWW at the density level of the upper halocline. Although this cold-core eddy contains nutrient-rich PWW and plays an important role in transporting nutrients from the Chukchi Sea shelf to the Canada Basin (Muench et al., 2000; Mathis et al., 2007), it hardly affects primary production (Nishino et al., 2011a). However, the warm-core eddies observed in this study substantially enhanced the primary production rate because they were located near the surface or at a shallower depth than the cold-core eddies. In fact, carbon, nitrate, and ammonium uptake rates of phytoplankton in the Canada Basin during our study would be about 43%, 73%, and 13% lower, respectively, if we excluded the stations affected by the warm-core eddies. Especially, the substantially high nitrate uptake rates of phytoplankton in the eddy region compared to neighboring non-eddy regions indicates that the warm-core eddies could lead to a significant increase in annual new production in the region.

The two warm-core eddies observed in this study were adjacent to each other. We could not identify the stage of the eddies, i.e., whether they were developing or coalescing with another anticyclone eddy. Generally, anticyclonic eddies cause a downwelling at the center of eddies (McGillicuddy and Robinson, 1997; Landry et al., 1998; Mizobata et al., 2002). Mizobata et al. (2002) reported that an anticyclonic eddy drove isopycnals downward, resulting in low nutrient and chlorophyll *a* concentrations at the center of the eddy. However, they found high chlorophyll *a* concentrations at the periphery and edge of the anticyclonic eddies that were caused by isopycnals that were tilted up and by cold nutrient-rich water being transported into the euphotic zone in the Bering Sea during summer 2000 and 2001 (Mizobata et al., 2002). In our study, a downwelling pattern that depressed the nitracline was identified at the centers of the left side eddy (Fig. 9). However, the largest feature was the shoaling of the nitracline between the two eddies. The upward nitracline (about 30–40 m) was much shallower than the average euphotic zone (about 50 m) at stations 10 and 13. In addition, there was more nitrate upward fluxes at stations 10 and 13 than non-eddy regions. Based on the vertical nitrate gradient ($\Delta NO_3^-/\Delta Z$, mmol m^{-4}; which was the difference in nutrient concentration over the vertical interval ΔZ of interest (Cota et al., 1987)) and the coefficient of vertical eddy diffusivity (Kz, cm^2 s^{-1}; which was estimated from an empirical equation determined by density gradients and nitrate gradients

below the mixed layer (King and Devol, 1979)), the estimated nitrate upward flux was 18.6 and 12.0 μmol NO_3 m^{-2} h^{-1} at stations 10 and 13 affected by warm-core eddies. These values were considerably higher than those in non-eddy regions (ranged from 0.7 to 6.0 μmol NO_3 m^{-2} h^{-1}). Thus, the high productivity in the eddy region could be due to increased nitrate upward flux, since there is the upwelling of nutrient-rich waters along steeply sloping isopycnals in the periphery of the eddies (Crawford et al., 2005). In addition, the movement of these eddies away from the ridge caused the shoaling of the nitracline because it is in deeper water and eventually the greater depth of the right side eddy played in its greater productivity. Consequently, these distinct eddy distributions enhanced the nitrate supply in the region, leading to the higher phytoplankton biomass and production rates than in the surrounding water.

It also appears that the phytoplankton productivity in the right side eddy is greater around the periphery, similar to other observations (Crawford et al., 2005; Whitney and Robert, 2002). Crawford et al. (2005) found that eddies entrained chlorophyll from an adjacent eddy located closer to the coast into the deep-sea region through the seaward advection of highly productive coastal waters in the outer rings of eddies. Whitney and Robert (2002) suggested that high phytoplankton biomass in outer ring of the eddy could be due to nutrients that advected upward and outward along upward-sloping isopycnals.

Nishino et al. (2011a) also found an unusually large surface-intensified warm-core eddy (approximately 100 km in diameter) in the southwestern Canada Basin during late summer/early fall in 2010. They reported that warm-core eddy contained considerably high ammonium concentrations (from 0.5 to 2 μM, with an average of 0.9 μM) compared with surrounding water (almost zero) at the same depths. Their findings indicated that the warm-core eddy supplied ammonium to the euphotic zone sustaining an ~30% higher biomass of picoplankton (< 2 μm) (Nishino et al., 2011a). However, we found that the nitrate supply by warm-core eddies resulted in high contributions of large phytoplankton (Fig. 10b). Unlike results from Nishino et al. (2011a), the mean ammonium concentration (0.6 ± 0.1 μM) in the euphotic zone of eddy regimes from our study was not largely different from that (0.4 ± 0.2 μM) in other stations of the Canada Basin. Thus, the supply of different nutrient types caused differences in the size compositions of phytoplankton between our study and that of Nishino et al. (2011a). Normally, small phytoplanktons depend largely on regenerated nitrogen such as ammonium, whereas large cells prefer nitrate for their growth (Probyn, 1985; Koike et al., 1986; Tremblay et al., 2000; Lee et al., 2008). Consequently, the warm eddies observed in our study largely affected the nitrate distribution and phytoplankton size composition, and generated high carbon and nitrogen uptake rates.

5. Conclusions

During the first Korean Arctic cruise onboard the Korean research icebreaker *ARAON*, we measured the carbon and nitrogen uptake rates of phytoplankton in the northeast Chukchi Sea and the western Canada Basin. The carbon uptake rates of phytoplankton in the region in 2010 were extremely low. In the northeast Chukchi Sea, regional and temporal differences might have caused the low production rate compared to the results of previous studies. The regions of high primary production in the Chukchi Sea are usually in the central and southern areas (Lee et al., 2007, 2013a), although the Chukchi Sea is well known as one of the very productive regions due to the nutrient-rich Pacific-water (Sambrotto et al., 1984; Springer and McRoy, 1993). In this study, we observed that the rate of primary production in the less studied northeast region is the lowest within the Chukchi Sea.

The low rate of primary production in the western Canada Basin might be explained by the dominance of small phytoplankton with a low uptake rate (Lee et al., 2013b). However, warm eddies could play an important role in the supply of nitrate to the euphotic zone and hence induce a high phytoplankton biomass and primary production rate locally in the Canada Basin. The Canada Basin in the Arctic Ocean is populated by significant numbers of small-scale eddies with diameters of 10–20 km (Manley and Hunkins, 1985). The frequent occurrence of eddies with the recent loss of sea ice (Kawaguchi et al., 2012) might enhance primary production rate in the Canada Basin. Thus, the effects of ocean circulation, such as by eddies and gyres, on primary production need to be continuously examined to better understand their roles in arctic marine ecosystems.

Acknowledgments

We thank the captain and crew of the *ARAON* for their outstanding assistance during the cruise. We are also grateful to Prof. Ho Kyung Ha of the Inha University and Dr. Hyoung Sul La of the Korea Polar Research Institute and Dr. Young Nam Kim of the Korea Marine Environment Management Corporation for providing CTD data and nutrient data. We gratefully acknowledge to Drs. Seung Hyun Son and Hyun- Cheol Kim for providing satellite data. In addition, we are grateful to the anonymous three reviewers who helped us make significant improvements to this manuscript. This work was supported by grants from the Korea-Polar Ocean in Rapid Transition (K-PORT; PM14040) program funded by the Ministry of Oceans and Fisheries, Korea. This study was also financially supported by the "2015 Post-Doc. Development Program" of Pusan National University.

References

Arrigo, K.R., van Dijken, G., Pabi, S., 2008. Impact of a shrinking Arctic ice cover on marine primary production. Geophys. Res. Lett. 35, L19603. http://dx.doi.org/10.1029/2008GL035028.

Carmack, E.C., Chapman, D.C., 2003. Wind-driven shelf/basin exchange on an Arctic shelf: The joint roles of ice cover extent and shelf-break bathymetry. Geophys. Res. Lett. 30 (14), 1778. http://dx.doi.org/10.1029/2003GL017526.

Carmack, E.C., Macdonald, R.W., Jasper, S., 2004. Phytoplankton productivity on the Canadian shelf of the Beaufort Sea. Mar. Ecol. Prog. Ser. 277, 37–50.

Comiso, J.C., Parkinson, C.L., Gersten, R., Stock, L., 2008. Accelerated decline in the Arctic sea ice cover. Geophys. Res. Lett. 35, L01703. http://dx.doi.org/10.1029/2007GL031972.

Cooper, L.W., Whitledge, T.E., Grebmeier, J.M., Weingartner, T.J., 1997. Nutrient, salinity and stable oxygen isotope composition of Bering and Chukchi Sea waters in and near the Bering Strait. J. Geophys. Res. 102 (C6), 12563–12573.

Cota, G.F., Prinsenberg, S.J., Bennett, E.B., Loder, J.W., Lewis, M.R., Anning, J.L., Watson, N.H.F., Harris, L.R., 1987. Nutrient fluxes during extended blooms of Arctic ice algae. J. Geophys. Res. 92 (C2), 1951–1962.

Cota, G.F., Pomeroy, L.R., Harrison, W.G., Jones, E.P., Peters, F., Sheldon, W.M., Weingartner, T.R., 1996. Nutrients, primary production and microbial heterotrophy in the southeastern Chukchi Sea: Arctic summer nutrient depletion and heterotrophy. Mar. Ecol. Prog. Ser. 135, 247–258.

Crawford, W.R., Brickley, P.J., Peterson, T.D., Thomas, A.C., 2005. Impact of Haida Eddies on chlorophyll distribution in the Eastern Gulf of Alaska. Deep Sea Res. Part II 52, 975–989.

Dugdale, R.C., Goering, J.J., 1967. Uptake of new and regenerated forms of nitrogen in primary productivity. Limnol. Oceanogr. 12, 196–206.

Gardner, W.D., Chung, S., Richardson, M.J., Walsh, I.D., 1995. The oceanic mixed layer pump. Deep Sea Res. Part II 42, 757–765.

Gosselin, M., Levasseur, M., Wheeler, P.A., Horner, R.A., Booth, B.C., 1997. New measurements of phytoplankton and ice algal production in the Arctic Ocean. Deep Sea Res. Part II 44, 1623–1644.

Hama, T., Miyazaki, T., Ogawa, Y., Iwakuma, T., Takahashi, M., Otsuki, A., Ichimura, S., 1983. Measurement of photosynthetic production of a marine phytoplankton population using a stable ^{13}C Isotope. Mar. Biol. 73, 31–36.

Hill, V.J., Matrai, P.A., Olson, E., Suttles, S., Steele, M., Codispoti, L.A., Zimmerman, R.C., 2013. Synthesis of integrated primary production in the Arctic Ocean: II. In situ and

remotely sensed estimates. Prog. Oceanogr. 110, 107–125. http://dx.doi.org/10.1016/j.pocean.2012.11.005.
Jackson, J.M., Carmack, E.C., McLaughlin, F.A., Allen, S.E., Ingram, R.G., 2010. Identification, characterization, and change of the near-surface temperature maximum in the Canada Basin, 1993–2008. J. Geophys. Res. 115, C05021. http://dx.doi.org/10.1029/2009JC005265.
Jones, E.P., Anderson, L.G., 1986. On the origin of the chemical properties of the Arctic Ocean halocline. J. Geophys. Res. 91, 10759–10767.
Kawaguchi, Y., Itoh, M., Nishino, S., 2012. Detailed survey of a large baroclinic eddy with extremely high temperatures in the Western Canada Basin. Deep Sea Res. Part I 66, 90–102. http://dx.doi.org/10.1016/j.dsr.2012.04.006.
King, F.D., Devol, A.H., 1979. Estimates of vertical eddy diffusion through the thermocline from phytoplankton nitrate uptake rates in the mixed layer of the eastern tropical Pacific. Limnol.Oceanogr. 24, 645–651.
Koike, I., Holm-Hansen, O., Biggs, D.C., 1986. Inorganic nitrogen metabolism by Antarctic phytoplankton with special reference to ammonium cycling. Mar. Ecol. Pro. Ser. 30, 105–116.
Krishfield, R.A., Proshutinsky, A., Tateyama, K., Williams, W.J., Carmack, E.C., McLaughlin, F.A., Timmermans, M.-L., 2014. Deterioration of perennial sea ice in the Beaufort Gyre from 2003 to 2012 and its impact on the oceanic freshwater cycle. J. Geophys. Res. Oceans 119, 1271–1305. http://dx.doi.org/10.1002/2013JC008999.
Landry, M.R., Brown, S.L., Campbell, L., Constantinou, J., Liu, H., 1998. Spatial patterns in phytoplankton growth and microzooplankton grazing in the Arabian Sea during monsoon forcing. Deep Sea Res. Part II 45, 2368–2523.
Lasternas, S., Agustı´, S., 2010. Phytoplankton community structure during the record Arctic ice-melting of summer 2007. Polar Biol. 33, 1709–1717.
Lee, S.H., Whitledge, T.E., 2005. Primary and new production in the deep Canada Basin during summer 2002. Polar Biol. 28, 190–197.
Lee, S.H., Whitledge, T.E., Kang, S.H., 2007. Recent carbon and nitrogen uptake rates of phytoplankton in Bering Strait and the Chukchi Sea. Cont. Shelf Res. 27, 2231–2249.
Lee, S.H., Whitledge, T.E., Kang, S.H., 2008. Carbon uptake rates of sea ice algae and phytoplankton under different light intensities in a landfast sea ice zone. Barrow, Alaska, Arctic 61, 281–291.
Lee, S.H., Stockwell, D., Whitledge, T.E., 2010. Uptake rates of dissolved inorganic carbon and nitrogen by under-ice phytoplankton in the Canada Basin in summer 2005. Polar Biol. 33, 1027–1036.
Lee, S.H., Joo, H.M., Liu, Z., Chen, J., He, J., 2012. Phytoplankton productivity in newly opened waters of the western Arctic Ocean. Deep Sea Res. Part II 81–84, 18–27.
Lee, S.H., Yun, M.S., Kim, B.K., Saitoh, S., Kang, C.-K., Kang, S.H., Whitledge, T.E., 2013a. Latitudinal carbon productivity in the Bering and Chukchi Seas during the summer in 2007. Cont. Shelf Res. 59, 28–36.
Lee, S.H., Yun, M.S., Kim, B.K., Joo, H.T., Kang, S.H., Kang, C.-K., Whitledge, T.E., 2013b. Contribution of small phytoplankton to total primary production in the Chukchi Sea. Cont. Shelf Res. 68, 43–50.
Legendre, L., Gosselin, M., 1996. Estimation of N or C uptake rates by phytoplankton using ^{15}N or ^{13}C: revisiting the usual computation formulae. J. Plankton Res. 19 (2), 263–271.
Li, W.K.W., McLaughlin, F.A., Lovejoy, C., Carmack, E.C., 2009. Smallest algae thrive as the Arctic Ocean freshens. Science 326, 539. http://dx.doi.org/10.1126/science.1179798.
Manley, T.O., Hunkins, K., 1985. Mesoscale eddies of the Arctic Ocean. J. Geophys. Res. 90, 4911–4930. http://dx.doi.org/10.1029/JC090iC03p04911.
Mathis, J.T., Pickart, R.S., Hansell, D.A., Kadko, D., Bates, N.R., 2007. Eddy transport of organic carbon and nutrients from the Chukchi Shelf: Impact on the upper halocline of the western Arctic Ocean. J. Geophys. Res. 112, C05011. http://dx.doi.org/10.1029/2006JC003899.
McGillicuddy, D.J., Robinson, A.R., 1997. Eddy-induced nutrients supply and new production in the Sargasso Sea. Deep Sea Res. Part I 44, 1427–1450.
McLaughlin, F.A., Carmack, E.C., 2010. Deepening of the nutricline and chlorophyll maximum in the Canada Basin interior, 2003–2009. Geophys. Res. Lett. 37, L24602. http://dx.doi.org/10.1029/2010GL045459.
Mizobata, K., Saitoh, S., Shiomoto, S., Miyamura, T., Shiga, N., Toratani, M., Kajiwara, Y., Sasaoka, K., 2002. Bering Sea cyclonic and anticyclonic eddies observed during summer 2000 and 2001. Prog. Oceanogr. 55, 65–75.
Muench, R.D., Gunn, J.T., Whitledge, T.E., Schlosser, P., Smethie Jr., W., 2000. An Arctic Ocean cold core eddy. J. Geophys. Res. 105, 23,997–24,006. http://dx.doi.org/10.1029/2000JC000212.
Nishino, S., Itoh, M., Kawaguchi, Y., Kikuchi, T., Aoyama, M., 2011a. Impact of an unusually large warm-core eddy on distributions of nutrients and phytoplankton in the southwestern Canada Basin during late summer/early fall 2010. Geophys. Res. Lett. 38, L16602. http://dx.doi.org/10.1029/2011GL047885.
Nishino, S., Kikuchi, T., Yamamoto-Kawai, M., Kawaguchi, Y., Hirawake, T., Itoh, M., 2011b. Enhancement/reduction of biological pump depends on ocean circulation in the sea-ice reduction regions of the Arctic Ocean. J. Oceanogr. 67, 305–314. http://dx.doi.org/10.1007/s10872-011-0030-7.
Nishino, S., Itoh, M., Williams, W.J., Semiletov, I., 2013. Shoaling of the nutricline with an increase in near-freezing temperature water in the Makarov Basin. J. Geophys. Res. 118, 635–649. http://dx.doi.org/10.1029/2012JC008234.
Parsons, T.R., Maita, Y., Lalli, C.M., 1984. A manual of chemical and biological methods for seawater analysis. Pergamon Press, New York p. 173.
Pickart, R.S., Stossmeister, G., 2008. Outflow of Pacific water from the Chukchi Sea to the Arctic Ocean. Chin. J. Polar Sci. 19, 135–148.
Probyn, T.A., 1985. Nitrogen uptake by size-fractionated phytoplankton populations in the southern Benguela upwelling system. Mar. Ecol. Prog. Ser. 22, 249–258.
Proshutinsky, A., Krishfield, R., Timmermans, M.-L., Toole, J., Carmack, E.C., McLaughlin, F.A., Williams, W.J., Zimmermann, S., Itoh, M., Shimada, K., 2009. Beaufort Gyre freshwater reservoir: state and variability from observations. J. Geophys. Res. 114, C00A10. http://dx.doi.org/10.1029/2008JC005104.
Robie, W.S., McRoy, C.P., Springer, A.M., 1992. Phytoplankton biomass distribution in the northern Bering Sea and southern Chukchi Sea. In: Nagel, P.A. (Ed.), Results of the Third Joint US–USSR Bering and Chukchi Seas Expedition (BERPAC). Summer 1988. US Fish and Wildlife Service, Washington, DC, pp. 123–127.
Sakshaug, E., 1980. Problems in the methodology of studying phytoplankton. In: Morris, I. (Ed.), The physiological ecology of phytoplankton. University of California Press, Berkeley, pp. 57–91.
Sambrotto, R.N., Goering, J.J., McRoy, C.P., 1984. Large yearly production of phytoplankton in the western Bering Strait. Science 225, 1147–1150.
Shimada, K., Kamoshida, T., Itoh, M., Nishino, S., Carmack, E.C., McLaughlin, F.A., Zimmermann, S., Proshutinsky, A., 2006. Pacific Ocean inflow: Influence on catastrophic reduction of sea ice cover in the Arctic Ocean. Geophys. Res. Lett. 33, L08605. http://dx.doi.org/10.1029/2005GL025624.
Springer, A.M., McRoy, C.P., 1993. The paradox of pelagic food webs in the northern Bering Sea-III. Patterns of primary production. Cont. Shelf Res. 13, 575–599.
Steele, M., Ermold, W., Zhang, J., 2008. Arctic Ocean surface warming trends over the past 100 years. Geophys. Res. Lett. 35, L02614. http://dx.doi.org/10.1029/2007GL031651.
Steele, M., Zhang, J., Ermold, W., 2010. Mechanisms of summertime upper Arctic Ocean warming and the effect on sea ice melt. J. Geophys. Res. 115, C11004. http://dx.doi.org/10.1029/2009JC005849.
Stroeve, J., Holland, M.M., Meier, W., Scambos, T., Serreze, M., 2007. Arctic sea ice decline: Faster than forecast. Geophys. Res. Lett. 34, L090501. http://dx.doi.org/10.1029/2007GL029703.
Subba Rao, D.V., Platt, T., 1984. Primary production of Arctic waters. Polar Biol. 3, 191–210.
Tremblay, J.E., Legendre, L., Klein, B., Therriault, J.C., 2000. Size-differential uptake of nitrogen and carbon in a marginal sea (Gulf of St. Lawrence, Canada): significance of diel periodicity and urea uptake. Deep Sea Res. Part II 47, 489–518.
Walsh, J.J., McRoy, C.P., Coachman, L.K., Goering, J.J., Nihoul, J.J., Whitledge, T.E., Blackburn, T.H., Parker, P.L., Wirick, C.D., Shuert, P.G., Grebmeier, J.M., Springer, A.M., Tripp, R.D., Hansell, D.A., Djenidi, S., Deleersnijder, E., Henriksen, K., Lund, B.A., Andersen, P., Muller-Karger, F.E., Dean, K., 1989. Carbon and nitrogen cycling within the Bering/Chukchi seas: source regions for organic matter effecting AOU demands of the Arctic Ocean. Prog. Oceanogr., 22; , pp. 277–359.
Whitney, F., Robert, M., 2002. Structure of Haida Eddies and their transport of nutrient from coastal margins into the NE Pacific Ocean. J. Oceanogr. 58 (5), 715–723.
Yamamoto-Kawai, M., McLaughlin, F.A., Carmack, E.C., Nishino, S., Shimada, K., Kurita, N., 2009. Surface freshening of the Canada Basin, 2003–2007: River runoff versus sea ice meltwater. J. Geophys. Res. 114 (C00A05), http://dx.doi.org/10.1029/2008JC005000.
Yang, J., 2009. Seasonal and interannual variability of downwelling in the Beaufort Sea. J. Geophys. Res. 114 (C00A14), http://dx.doi.org/10.1029/2008JC005084.
Yun, M.S., Chung, K.H., Zimmermann, S., Zhao, J., Joo, H.M., Lee, S.H., 2012. Phytoplankton productivity and its response to higher light levels in the Canada Basin. Polar Biol. 35, 257–268.
Yun, M.S., Whitledge, T.E., Gong, M., Lee, S.H., 2014. Low primary production in the Chukchi Sea shelf, 2009. Cont. Shelf Res. 76, 1–11.